Marine Geology 256 (2008) 36–48

Contents lists available at ScienceDirect

Marine Geology

journal homepage: www.elsevier.com/locate/margeo

Spatio-temporal variability in suspended particulate matter concentration and the role of aggregation on size distribution in a coral reef lagoon

Aymeric Jouon [a,b,*], Sylvain Ouillon [a,c], Pascal Douillet [a], Jean Pierre Lefebvre [a], Jean Michel Fernandez [a], Xavier Mari [a], Jean-Marie Froidefond [b]

[a] IRD, BP A5, 98848 Nouméa cedex, New Caledonia
[b] Université de Bordeaux, CNRS, UMR 5805, Bordeaux, F-33000, France
[c] LEGOS/OMP, Université de Toulouse, UMR 5566, 14 avenue Edouard Belin, 31400 Toulouse, France

ARTICLE INFO

Article history:
Received 30 January 2008
Received in revised form 16 September 2008
Accepted 28 September 2008

Keywords:
suspended particles
optical backscattering
beam attenuation
particle size distribution
flocs
marine aggregates
coral reef
New Caledonia

ABSTRACT

This paper presents the concentration and size distribution of suspended particles in the South-West Coral reef lagoon of the island of New Caledonia. Data are provided by filtration techniques, Optical BackScattering (OBS) measurements and in situ laser diffraction particle sizing. The concentration of suspended particles increased from reef to land. A bottom nepheloïd layer occurred over the entire lagoon, and was more distinct on the nearshore area. Small particles were more abundant in the bottom nepheloïd layer than in the overlying water column. The concentration of suspended particles showed more variability over space than over time. Conversely, the particle size distribution of suspended particles showed more variability at a given location over a month (time variability) than at a given moment over the lagoon (space variability). Analysis showed that aggregates represented a large fraction of suspended particles. Microscope visualization and chemical analysis of a sample suggest the inclusion of a transparent exopolymeric matrix. The relative abundance of aggregates over suspended particle volume concentration was found to increase as the quantity of suspended particle decreased. The spatial distribution of the relative abundance of aggregates suggests more aggregates proximal to coral reefs. The high concentration of aggregates at low turbidity and the spatial distribution of the relative abundance, infer that aggregation is induced by the presence of organic ligands. Unlike optical backscattering and light attenuation measurements that are size sensitive measurements of suspended particle concentration, in situ laser diffraction particle sizing provides a relevant optical measurement of suspended particulate matter in such an aggregate-dominated system.

1. Introduction

Suspended particulate matter (SPM) is a key vector for minerals, organic matter, nutrients and pollutants cycling in aquatic ecosystems. The amount, variability and fate of SPM force many biological processes. High turbidity modifies coral reef development by limiting light penetration by compressing the depth range over which coral can flourish (Hayward, 1982; Rogers, 1990; Hopley, 1994; Hoitink, 2004), and sedimentation inhibits coral recruitment (Babcock and Davies, 1991; Fabricius et al., 2003). On the other hand, coral abundance also induces changes in the SPM field characteristics. For example, on Eniwetok Atoll, Johannes (1967) observed a marked increase in the concentration of suspended particulate organic aggregates when oceanic waters crossed the windward coral reef and entered the lagoon. Benson and Muscatine (1974) highlighted the importance of coral mucus within SPM. By mixing turbid plume water with unfiltered coral reef water in equivalent ratio, Wolanski et al. (2003a) observed a rapid aggregation of particles leading to the formation of large aggregates. Wild et al. (2004) reported the occurrence of specific aggregation processes related to the production of mucus by corals, defining coral mucus as “a trap for particles” and as “an efficient energy carrier”.

The concentration of SPM is usually assessed by measuring the dry weight of particles. In numerous studies (e.g. Creed et al., 2001; Fugate and Friedrichs, 2002; Hoitink, 2004; Voulgaris and Meyers, 2004), turbidity measurements and mass concentration of SPM are directly linked, thus providing an estimate of naturally occurring SPM concentration. However, characterization of the SPM field also requires the determination of particle size distributions (PSD). Measuring the natural effective particle size distribution (EPSD) and the absolute particle size distribution (APSD, after disaggregation), is required in order to assess the importance of aggregation processes (Williams et al., 2007). APSD can be measured in the laboratory by

* Corresponding author. Université de Bordeaux, CNRS, UMR 5805, Bordeaux, F-33000, France. Tel.: +33 5 61 33 29 02.
E-mail addresses: a.jouon@epoc.u-bordeaux1.fr (A. Jouon), sylvain.ouillon@ird.fr (S. Ouillon), douillet@noumea.ird.nc (P. Douillet), jplefeb@noumea.ird.nc (J.P. Lefebvre), fernand@noumea.ird.nc (J.M. Fernandez), mari@noumea.ird.nc (X. Mari), jm.froidefond@epoc.u-bordeaux1.fr (J.-M. Froidefond).

0025-3227/$ – see front matter © 2008 Elsevier B.V. All rights reserved.
doi:10.1016/j.margeo.2008.09.008

sieving methods, Coulter Counter, and laser sizer technology. On another hand, EPSD measurements, which require aggregates to remain intact during analysis (Gibbs, 1982), have to be performed *in situ*. Laser-based technology devices, such as Cilas and Sequoia LISST instruments, use the principle of diffraction of a laser by particles to perform a non intrusive measurement of the volume concentration of suspended particles according to their size. The EPSD can thus be monitored. The straightforward innovation brought in this study is the measurement of EPSD in a coral reef lagoon.

The objectives of this study are: (1) to compare *in situ* parameters derived from LISST-100X to other parameters used to describe SPM, such as turbidity and light attenuation; (2) to describe time, space and depth variability of SPM and EPSD; (3) to estimate the amount of aggregates from the comparison between APSD and EPSD; and, (4) to discuss the importance of aggregation processes in a coral reef lagoon. Suspended aggregates have been described in various marine environments (Gentien et al., 1995; Fugate and Friedrichs, 2003), and are a major constituent of suspended particles (Gibbs and Wolanski, 1992; Droppo, 2001). However, to our knowledge, no paper has reported the use of an *in situ* laser particle sizer nor the description of effective particle size distribution in a coral reef environment.

2. Study area

New Caledonia is a tropical island surrounded by a lagoon of 22 200 km^2, located in the Western Pacific, 1500 km east of Australia. Over fifty percent of the population of New Caledonia (231 000 people) reside in the city of Nouméa, located on the southwest coast of the island (Fig. 1). Nickel mining is the major economic resource of New Caledonia. Over the last century, open-cast mining have increased the load of terrigenous inputs into the lagoon (Wodzicki, 1981; Bird et al., 1984; Ellison, 1999; Fernandez et al., 2006).

The lagoon area surrounding Nouméa is often referred as the "south-west lagoon of New Caledonia" (SLNC). The SLNC is a relatively shallow shelf (average depth 17.5 m), with a width varying from 5 km (northern limit) to 40 km (southern limit). The lagoon is fed by oceanic waters which stream through the passes and shoal over the barrier reef induced by breaking of oceanic waves (Bonneton et al., 2007). The e-flushing time of water masses – a residence time which corresponds to the renewal of 37% (1/e) of water – is 11.4 days in the SLNC in the case of averaged tide and trade wind conditions (Jouon et al., 2006).

Hydrodynamic studies based on the coupling of a 3D numerical model with *in situ* measurements showed that tide and wind were the major forcings of hydrodynamics on the SLNC. The tide is semi-diurnal with a diurnal inequality. Amplitudes (maximum of 1.8 m, minimum of 0.3 m) and phase-lags of the tide increase from south to north. M2 currents are maximum in the south (of the order 0.2 m s^{-1}) and in the passes. S2 amplitudes increase from south to north but slower than M2 (Douillet, 1998). The flow is globally oriented from SE to NW in the open part of the lagoon and towards the land inside the bays. The ebb is mostly opposite direction of the flow, leading to low intensity of tidal residual circulation. The most frequent scenario of wind blowing on the SLNC is a trade wind regime (70% of time). Trade winds come from the South-East and their average intensity is 8 m s^{-1}. Currents generated by the friction of wind over the SLNC are oriented from SE to NW, and the order of magnitude of wind generated currents is 0.1 m s^{-1} (Douillet et al., 2001). Despite the lower intensity of wind generated currents compared to tide generated currents, wind generated circulation plays a leading role in residual circulation. Wind generated currents reach higher intensities on the reef side of the lagoon where wind is not slowed by land topography. The renewal of water masses (local e-flushing times) is quicker on the barrier reef side (less than one week) of the lagoon than closer to the main land (more than a month) (Jouon et al., 2006).

Recent studies have shown the significant influence of residence time on the distributions of biological and geochemical parameters. Mari et al. (2007) proved that the efficiency of the transformation of dissolved organic matter to Transparent Exopolymeric Particles (TEP) and the TEP turnover rate dropped drastically when the residence time increased from 0 to 50 days. Torréton et al. (2007) showed that the concentration of silicate, chlorophyll a and bacterial biomass production present high correlations with flushing indices. Migon et al. (2007), focusing on the dissolved and particulate concentrations of Cr, Ni and Zr on the SLNC, state that "residence time is a key parameter in the control of elemental concentrations in the lagoon waters". As a consequence, the spatial variability of these biological and geochemical parameters is also governed by a reef to land gradient.

A hydrologic study of the variability in salinity and temperature in the SLNC showed that seasonal and interannual variations in salinity

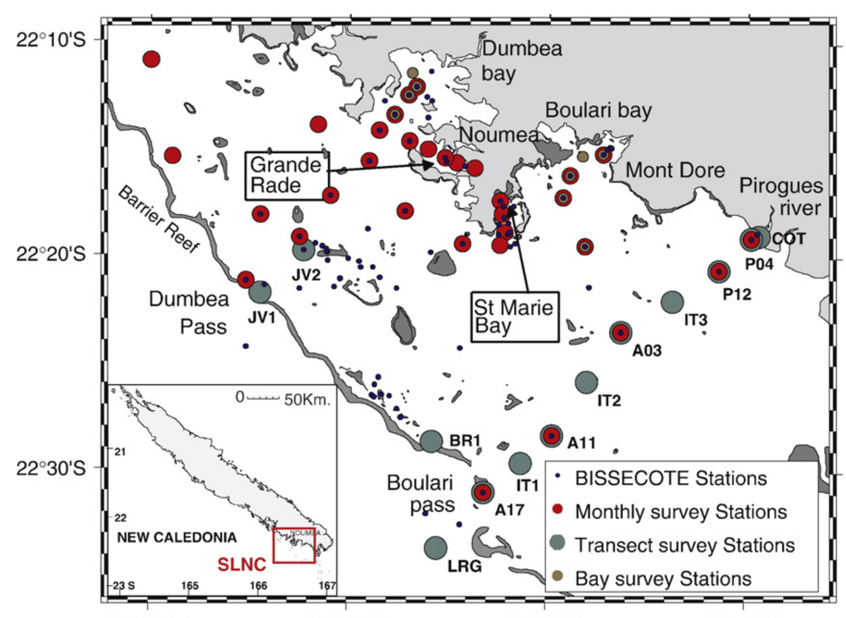

Fig. 1. Distribution of sampling stations during different surveys within the Southwest Lagoon of New Caledonia (SLNC).

are amplified nearshore. The temperature was proved to be warmer in bays than in the open lagoon during summer, this thermal gradient is reversed during winter (Ouillon et al., 2005).

The spatial variability of benthic cover roughly coincides to a reef to land gradient of biogenic to terrigenous sediments (Clavier et al., 1995). While terrigenous silicate mud is dominant on the land side of the lagoon, biogenic calcareous sediment is almost exclusively on the barrier reef side of the SLNC.

Despite terrestrial runoffs, which episodically affect the near-shore areas of the SLNC, the concentration of SPM is low (ca. 1 mg L^{-1}). The SPM encompasses particles such as bacteria, phytoplankton, organic detritus, zooplankton, aggregates and inorganic particles. The relative abundance of solid particles and of particulate organic matter in the SPM strongly varies (3 to 65%) in the SLNC (Mari et al., 2007). The comparison of sediment transport modeling and remotely sensed data showed that the major feature of the turbidity distribution on the SLNC is a barrier reef to land positive gradient (Ouillon et al., 2004).

3. Material and methods

3.1. Material

In this paper, a highly sensitive new generation instrument (LISST-100X) was used *in situ* to quantify SPM and EPSD in low SPM waters (down to ca. 0.2 mg L^{-1}). This study uses approximately 500 *in situ* measurements (i.e. LISST and Conductivity-Temperature-Depth-CTD-profiles). The LISST-100X was also used in laboratory to determine the APSD on a few characteristic sampling locations (11 APSD).

3.1.1. Lisst-100x

An *in situ* Laser Scattering and Transmissometry device (LISST-100X; Sequoia Scientific Inc.) was used. The LISST-100X provides the distribution of particle volume concentration in 32 size classes logarithmically spaced within the range 1.25–250 µm (LISST type B) and the beam attenuation coefficient (*c* at 670 nm, hereafter denoted c670 and expressed in m^{-1}) over an optical pathlength (*l*) of 5 cm.

The particle size distribution (PSD) is derived from the laser diffraction technology. The measurement principle used by LISST-100X is based on the application of Mie's theory. Measurement principles, calibration and validation procedures of LISST are detailed in Traykovski et al. (1999) and Agrawal and Pottsmith (2000).

3.1.2. Optical backscattering sensor (OBS)

Numerous studies have used optical backscattering sensors to assess total SPM concentration through turbidity measurements (e.g. Creed et al., 2001; Fugate and Friedrichs, 2002; Hoitink, 2004; Voulgaris and Meyers, 2004). In this study, a Seapoint OBS sensor (λ=880 nm) connected to a Seabird SBE19 CTD probe was used. The sensor was factory-adjusted for consistent response to Formazin Turbidity Standard. The calibration of backscattered light intensity to the mass concentration of SPM is done experimentally and is usually described by a linear relationship (Hoitink, 2004). OBS sensitivity was shown to be around 1 FTU for 1 mg L^{-1} in some coastal environments (Larcombe et al., 1995; Wass et al., 1997; Bunt et al., 1999; Jin et al., 2001) but requires a calibration per site and per OBS.

3.1.3. Mass concentration determined by filtration

Water sampling was performed using a 6-L Niskin bottle at 3 m depth, and the *in situ* data were considered to correspond to the average of coincident optical probe data recorded from 1 m above to 1 m below this sampling depth. Seawater was filtered in the laboratory on pre-weighted 1-µm Nuclepore polycarbonate filters in order to fit the LISST-100X sensing window (i.e., >1.25 µm). Weight measurements of filters were performed using a balance with a precision of ±0.001 mg.

3.1.4. Disaggregation and individual particles

APSD measurements were performed as follows: the material retained on filters was resuspended in a solution of 0.01 M $Na_4P_2O_7$ and sonicated for two minutes in a Sonifier, following Mikkelsen and Pejrup (2000); the resulting solution was channeled in a closed circuit entrained by a peristaltic pump through the LISST-100X measurement chamber. Water flow rate was adjusted to prevent settling and the production of bubbles, and a magnetic stirrer was activated in the sampling chamber to prevent particle settlement.

3.2. Sampling strategy

The data collection consisted of LISST-100X profiles in the water column (at 1 Hz) and Seapoint OBS profiles (4 Hz) connected to a Seabird CTD. Only the downcast data were considered to avoid disturbance caused by resuspension of particles when instruments reach the seabed.

The data considered in this study were collected over a series of three surveys (Fig. 1):

1. A monthly 30-hour survey was conducted from March to September 2005 and in February 2006. This survey offered a quasi-synoptic selection of 31 stations within the SLNC. The collected data were used to assess the time and space variability of SPM and EPSD.
2. Transects focusing on open water to coast gradients were performed simultaneously to the monthly surveys as well as in December 2005 and March 2006. The data collected were used to assess the importance of aggregates in the EPSD by comparing APSD and EPSD.
3. 158 coincident CTD and LISST profiles were performed on a substrate variability strategy in January and February 2006 (Bissecote and “bay survey” stations in Fig. 1). These data were used to map the mean SPM and EPSD distribution on the SLNC.

Water was sampled at approximately one out of every three sampling stations during these cruises. Filtering and weighting were performed at 137 stations.

3.3. Data analysis

3.3.1. SPM volume concentration (SPMVC)

LISST software provides the volume concentration per size class. The total SPM volume concentration (SPMVC, expressed in µL L^{-1}) is calculated using the relationship described by Traykovski et al. (1999):

$$SPMVC = \sum_i C_{vol,i} \tag{1}$$

where $C_{vol,i}$ is the volume concentration in the *i*th LISST size class.

Despite the smoothing parameter used to compute the particle volume concentration distribution (Traykovski et al., 1999), LISST-100X derived data was highly variable on classes #1 and #32 even when measuring continuously the same sample. Using another version of LISST (sensing range of 1.25 to 500 µm) Traykovski et al. (1999) reported a lack of accuracy of the instrument for the biggest (>250 µm) and the smallest (<5 µm) particles of the sensing range. This high variability of the signal is likely due to the presence of particles smaller and coarser than the measured size range, which affects the estimated size distribution (Traykovski et al., 1999; Agrawal and Pottsmith, 2000; Mikkelsen and Pejrup, 2000; Fugate and Friedrichs, 2002; Voulgaris and Meyers, 2004; Mikkelsen et al., 2005). Due to this uncertainty, these two bins were excluded in the SPMVC calculation (*i* ranges from 2 to 31 in Eq. (1)). This exclusion may lead to an underestimation of the SPMVC by not taking into account the volume concentration of particles in the size range of excluded bins. However, excluding some bins from the computation is a solution that has already been used in Curran et al. (2007) in which the exclusion concerns 6 bins of their LISST-100 data.

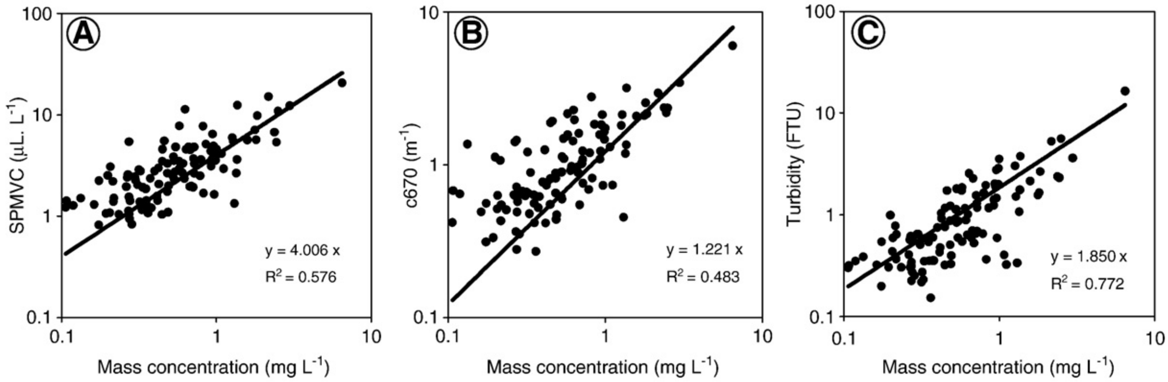

Fig. 2. Comparisons between optical parameters and SPM mass concentrations at 137 stations: (A) total volume concentration vs mass concentration. (B) beam-attenuation at 670 nm vs mass concentration. (C) turbidity vs mass concentration.

In order to assess the potential link between the various measurements of the quantity of suspended particles, turbidity, c670 and SPMVC were examined as proxies for mass concentration (Fig. 2). Only stations where all these parameters were measured at the same time and depth, were considered (N=111).

Mean values of SPMVC were calculated over the water column at stations where monthly measurements were performed. These stations were sampled 8 times to get mean values that were not influenced by the time variability of SPMVC. Despite considerable efforts to make the sampling scheme as widespread on space and time as possible, the mean display of SPMVC on the SLNC may not be completely representative. As the sampling was conducted over a year, the interannual variability of SPMVC cannot be taken into account in the results of this study. Rendering the mean display of SPMVC on the SLNC would require more data sampled throughout the year over multiple years. However, the climatic conditions over the year of sampling were similar to a neutral average local climatic year (i.e. neither an El-Niño nor a La Nina event). The produced data can therefore be considered to yield the major tendencies of the mean display of SPMVC on the SLNC.

3.3.2. Particle size distribution (PSD)

The distribution of volume concentration of particles given by LISST-100X is the cumulative distribution discretised over the continuous spectrum of size classes. Therefore, the data given by LISST-100X is instrument dependent as it depends on the chosen discretisation of the continuous size spectrum. A volume concentration distributed on particle size can alternatively be expressed per unit volume and per unit bin width (Mobley, 1994; Boss et al., 2001a,b).

In order to assess the volumetric PSD, data were normalized by the extent of each class to obtain an instrument independent particle size distribution following:

$$C_{vol}(size(i)) = \frac{C_{vol,i}}{\max(range(i)) - \min(range(i))} \tag{2}$$

where *size (i)* is the median diameter of particle size class i and *range (i)* is the particle size range on which extends the i-th class. The resulting data are expressed in µL L^{-1} µm^{-1}.

Further on, the volume concentration of each particle size was divided by the SPMVC in order to provide a particle size distribution independent of the total amount of particles, following:

$$C_{vol,rel}(size(i)) = \frac{C_{vol} size(i)}{SPMVC} = \frac{C_{vol} size(i)}{\sum_i C_{vol,i}}. \tag{3}$$

$C_{vol,rel}$ (*size(i)*) is called hereafter the relative volumetric PSD. This representation allows the comparison of a PSD from one size to another as well as from one PSD to another.

3.3.3. Junge's parameter

Assuming the particles are spherical (as in Mie's theory used to invert the signal in LISST data processing), it is possible to compute the PSD of the number of particles per size *(n(size(i)))* following:

$$n(size(i)) = \frac{C_{vol}(size(i))}{\left(\frac{4}{3}\pi\left(\frac{size(i)}{2}\right)^3\right)}. \tag{4}$$

In oceanic waters, this distribution generally fits a logarithmic curve (Mobley, 1994):

$$n(D) = K_1 D^{-s} \tag{5}$$

where K_1 is a constant, D is the diameter of particles and s is the slope of the best fitted linear relationship between *log n(D)* and *log D*. s is called the Junge parameter. It is a synthetical parameter characterizing the particle size distribution: high values correspond to SPM dominated by fine particles or aggregates while low values correspond to SPM dominated by macroflocs. s=4 generally fits the distribution of biological particles as they are encountered in open ocean waters (Mobley, 1994). The Junge parameter is useful for calculations of radiative transfer in the water column and their applications to remote sensing (e.g. Forget et al., 1999).

3.3.4. Coefficient of variation

The standard deviation of a given parameter x is hereafter calculated following:

$$\text{stdev}\ (x) = \left[\frac{1}{(n-1)}\sum_{i=1}^{n}(x_i - \bar{x})^2\right]^{1/2} \tag{6}$$

where $\bar{x}$ is the mean value. The ratio of the standard deviation of x on its mean value is called coefficient of variation and is used in this study as a proxy for the variability of parameters over space and time. Expressed in percentage, the coefficient of variation is given by:

$$\text{Cv} = 100\frac{stdev(x)}{\bar{x}}. \tag{7}$$

In itself, the coefficient of variation provides no indication of the cause of the variability (e.g. wind-wave action or river discharge). However, it is an interesting broad indicator of variability, which is frequently used for example in hydrology (Achite and Ouillon, 2007).

In an attempt to discriminate temporal and spatial variations of SPMVC, the variation coefficients over space and time were calculated. Computations were performed over 23 stations all sampled 8 times at monthly intervals. Mean, standard deviation and coefficient of variation were calculated from the spatial (resp. temporal) variations of SPMVC for each cruise (resp. station). A coefficient of variation over space was calculated for each field campaign, and the 8 values were then averaged. A coefficient of variation over time was calculated for each station, and these 23 values were then averaged providing a mean coefficient of variation over time.

We do not claim to capture the complete time variability with 8 dates. Such an attempt would require more sampled data, notably during storm episodes. However, the concerned variation coefficient can be considered as an indicator of the time variability of SPMVC field under recurrent and unexceptional weather conditions. Furthermore, computing a variability indicator over space should strictly use data sampled synchronously over space. Unfortunately, this pre-requisite is not realizable, as it would require as many LISST probes as the number of stations that were considered. Thus, the variation coefficient computed over space inevitably includes a small amount of time variability, the scale of which is assessed in the results of this study.

3.3.5. State of aggregation indicator

The state of aggregation of SPM was described through the ratio of the volume concentration contained in aggregates over SPMVC, the total volume concentration. While all sizes in the EPSD probably include a certain amount of aggregates, only a fraction of the particle sizes are proved to be entirely composed of aggregates. The ratio of the volume concentration contained in these “all aggregate sizes” to the SPMVC, which is used in this study, is thus a low estimate of the real state of aggregation.

4. Results

4.1. Suspended particulate matter volumetric concentration

4.1.1. Regressions between measurements

4.1.1.1. Optical measurements and mass concentration. 111 stations with concurrent measurements of turbidity, c670 and SPMVC, correspond to values in the ranges of 0.2 to 16.2 FTU for turbidity, 0.12–6.0 m^{-1} for c670, 0.48–20.5 µL L^{-1} for SPMVC and 0.01–6.48 mg L^{-1} for mass concentration.

The determination coefficient between turbidity and mass concentration (r^2=0.77, Fig. 2A) was better than the one obtained for volume concentration (r^2=0.58, Fig. 2B) and c670 (r^2=0.48, Fig. 2C). Fig. 2 shows dispersed patches of points for low mass concentration values (<1 mg L^{-1}).

4.1.1.2. Measurements per LISST size class versus other parameters. The correlations between turbidity, c670 and mass concentration, and the volume concentration $C_{vol,i}$ in each LISST-100X size class are shown in Fig. 3.

$C_{vol,i}$ showed a higher correlation to mass concentration than to turbidity and c670 for each particle size. The relation between volume concentration and mass concentration is more straightforward than the relations between volume concentration and other optical measurements of SPM. Correlation coefficient between $C_{vol,i}$ and mass concentration was over 0.7 for all size classes except for the size class #1, and for size class #26 (~86 µm) and above. $C_{vol,i}$ was globally better correlated with turbidity than with c670.

Interestingly, the correlation between volume concentration and any optical parameter decreased with increasing diameter above class #26.

The volume concentration of particles <3 µm (below class #6) was not as strongly correlated to any optical parameter than particles from size classes #6 to #15. The highest correlations between turbidity and volume concentration were found for classes #6 to #18, i.e. for particles with equivalent diameters between 3 and 23 µm. The highest correlations between c670 and volume concentration were found at two intervals, which extend from classes #6 to #9 (ca. 3 to 5 µm) and from #22 to #26 (ca. 40 to 100 µm). Further observations concerning the second size range showing stronger correlation to the beam attenuation are given in section 5 below.

4.1.2. Mean spatial distribution of suspended particulate matter volumetric concentration

Mean SPMVC values were low (<7.5 µL L^{-1}, Fig. 4). A reef-to-land gradient is visible. The volume concentration was highest at the head of bays, and peaked in a bay strongly impacted by urban inputs, i.e. the bay of Sainte-Marie (see location in Fig. 1). SPMVC was also high in the Dumbea Bay. Inside Dumbea Bay, the Bay of Grande Rade is characterized by intense industrial activity, leading to industrial inputs of particles to the SLNC (e.g. polder construction with scoria, penetration of flying ashes from blast-furnace by deposition at the sea surface). The third zone with relatively high SPMVC was the bay of Boulari, which receives terrestrial inputs from La Coulée River (Fernandez et al., 2006).

The analysis of vertical profiles shows that SPMVC, turbidity and beam attenuation coefficient tend to increase within the benthic bottom layer (a typical example is given in Fig. 5).

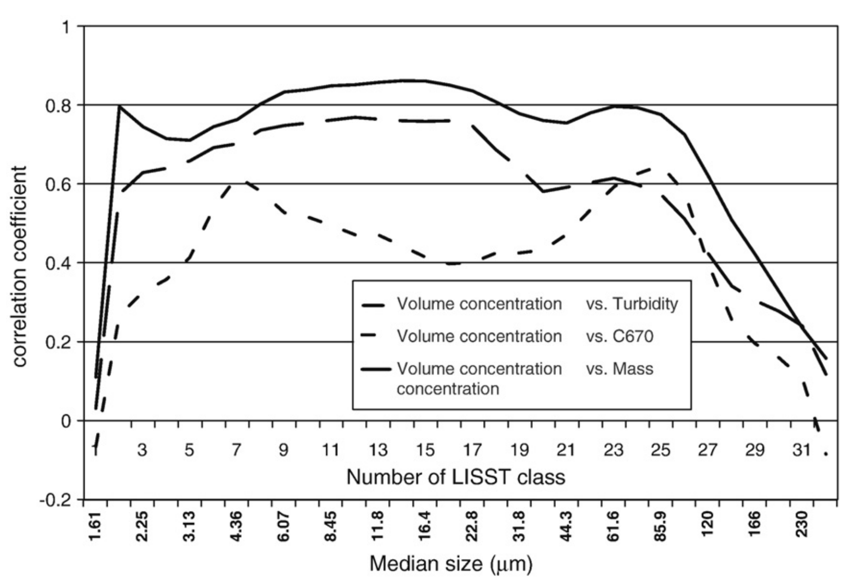

Fig. 3. Correlations of and mass concentration (N=111), turbidity and c670 (N=36043) with SPM volume concentration per LISST size class in the SLNC.

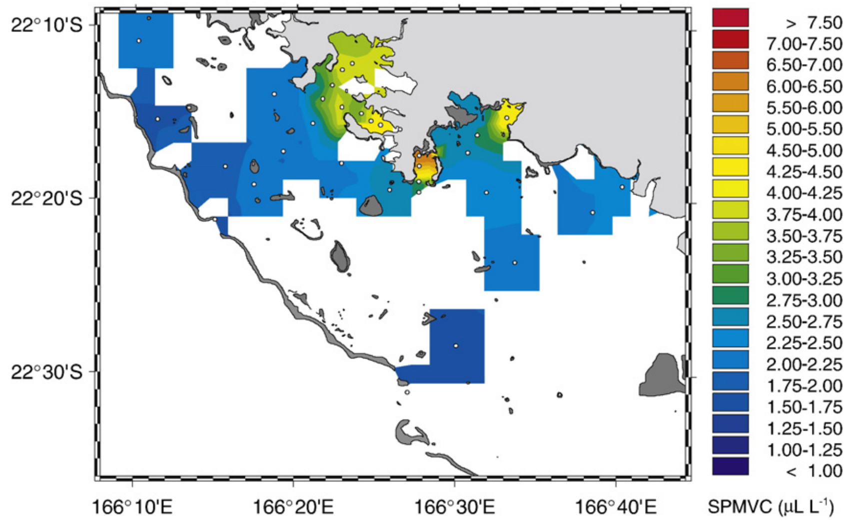

Fig. 4. Mean SPM volume concentration (in μL L^{-1}) in the SLNC. Averaging was performed over depth and over 8 field campaigns.

4.1.3. Space and time variability

The mean coefficient of variation of SPMVC over space is 63%. The mean coefficient of variation of SPMVC over time is 26%.

In order to assess the order of magnitude of SPMVC time variability that is included in the variation coefficient computed over space, the variation coefficient of SPMVC over time was computed for two stations B08 and A11 during two successive tidal cycles (see locations in Fig. 1). These two stations were sampled every 30mn during 24 h. At B08 the 24 h variation coefficient was found to be 12% and at A11 it was 38%. The entering of oceanic waters through the Boulari Pass was mainly responsible for the high value of variation obtained at station A11. However, knowing that the sampling has been performed randomly regarding forcing conditions and that the variation coefficient of SPMVC over space is computed over the SPMVC field averaged over sampling events, we presume that the computed 24 h variation coefficient represents a high estimate of the time variation included in the variation coefficient of SPMVC “over space”.

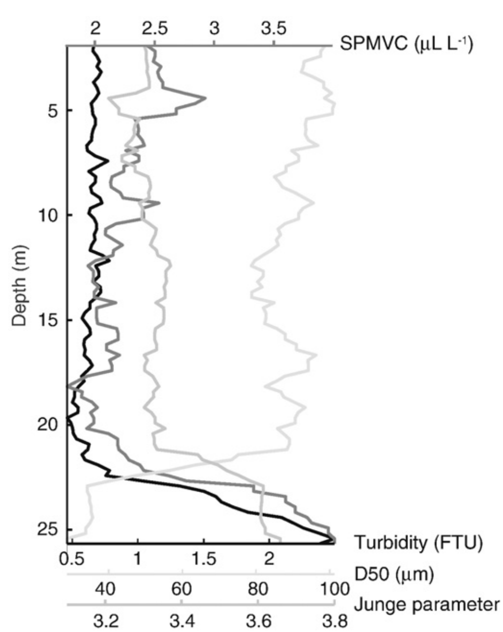

Fig. 5. Typical depth-profiles of SPMVC, turbidity and c670 within the SLNC (station B24, 2006/01/22).

From our measurements, the SPMVC varies 63% over the SLNC and varies 26% over time around its time and space averaged value. According to these indicators of variability, space variability of suspended particles concentration is higher than its time variability.

4.2. Particle size distribution

4.2.1. Effective particle size distribution (EPSD)

4.2.1.1. Several descriptions of EPSD. In order to compare PSDs, distributions of $C_{\mathrm{vol,i}}$ and C_{vol} (*size*(i)) at one station from the surface to the bottom are shown as an example in Fig. 6. The volume concentrations of particles contained in small size classes have relatively higher values when the LISST data ($C_{\mathrm{vol,i}}$) are turned into C_{vol} (*size*(i)). This change is due to the logarithmic spacing of particle size classes of LISST data. Profiles presented in Figs. 5 and 6 are typical of those encountered in the whole SLNC. The fluctuations of large particles volume concentration is better represented using $C_{\mathrm{vol,i}}$ (Fig. 6A) whereas C_{vol} (*size*(i)) representation is better suited to render fluctuations of volume concentration of smaller particles (Fig. 5b). C_{vol} (*size*(i)) is hereafter referenced as the EPSD distribution when the measurements were performed *in situ*.

EPSD changes or variations can be studied through the use of synthetic parameters, such as the median particle size diameter and the Junge parameter which can be computed at every water depth or averaged over the profile. The particles are typically finer in the bottom nepheloid layer than in the upper mixed layer (Fig. 5). The shifts of the Junge parameter curve are shown to be opposite of the ones of SPMVC (Fig. 5).

4.2.1.2. Mean EPSD over the SLNC. The normalized value of *EPSD*, namely $C_{vol,rel}$ (*size(i)*), was averaged over all the measurements performed within the SLNC so as to provide a normalized particle volume concentration distribution representative of the SLNC (Fig. 7). Volume concentration was the highest for particles with a diameter around 6 μm. The lowest volume concentration was obtained for particles within the 1.9–2.6 μm size range. As previously discussed, the high volume concentration recorded for particles of 1.6 μm diameter may be an artefact. The curve describing the mean relative volume concentration distribution decreased from the maximum reached around 6 μm to the highest particle sizes. This decrease, as shown on the semi-log plot on Fig. 7, displays four loose modes from 6 μm to 60 μm. A second distinct mode appears for particles of size ranging from 60 to 120 μm.

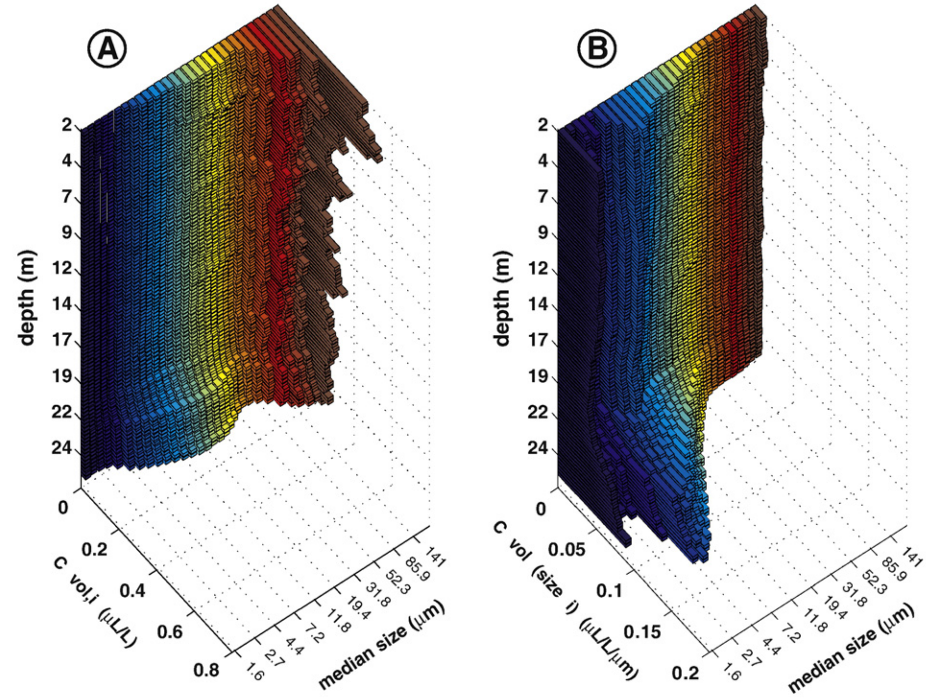

Fig. 6. Example of LISST-100X (A) profile and (B) its conversion into particle size distribution profile (station B24, 2006/01/22, see Fig. 5).

4.2.1.3. Space and time EPSD variability. The standard deviation of $C_{vol,rel}$ (size(i)) is generally higher in time than in space (Fig. 7). The EPSDs were more similar for different stations sampled during the same campaign than those obtained from different samplings at the same station. Both curves of standard deviations show oscillations. The major peak is reached for particles of 3.7 µm diameter. The standard deviation curves rapidly decreased to a low value for particles of 7 µm and shows successive peaks and troughs up to the upper end of the distribution. The last significant peak is observed where the space and time averaged normalized EPSD shows also a peak for particles between 60 and 120 µm diameter.

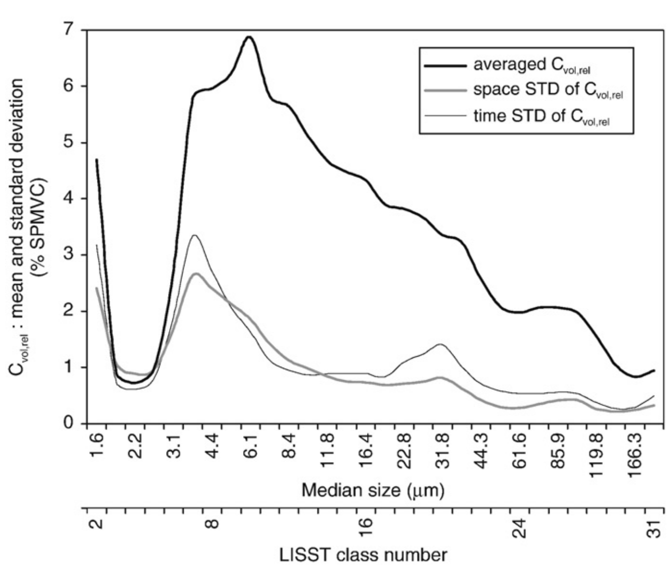

Fig. 7. Normalized volume concentration distribution on the SLNC, standard deviation in space and standard deviation in time.

4.2.1.4. Junge parameter distribution. Junge parameters extend from 2.6 to 3.5 (Fig. 8). These values are lower than the theoretical open sea value of 4 (Mobley, 1994). Large particles are relatively more abundant in SLNC waters than in the open ocean. The 2D Junge parameter distribution shows a distinct gradient from high values at the reef decreasing to the coast. Small particles represent a larger fraction of SPM at the head of the bays than near the barrier reef or around the coral islands. Separating near-seabed data from the rest of the profile emphasizes the relative prevalence of small particles in the bottom nepheloïd layer (Fig. 8B).

4.2.2. Absolute particle size distribution (APSD)

4.2.2.1. Identification of aggregates. In order to identify the presence of aggregates, we compared the EPSD (potentially with aggregates) to APSD of particles sampled at the same stations. Disaggregating experiments were achieved on samples made during a transect survey from Boulari Pass to the Pirogues River mouth, and at two stations sampled on a different day (JV1, JV2, see locations in Fig. 1).

Fig. 9 shows EPSDs (Fig. 9A) and APSDs (Fig. 9B) at 11 stations. All disaggregated samples had similar APSD, suggesting similar sizes for the grains constituting the aggregates. EPSDs are more scattered. This demonstrates the high amount of aggregates among suspended particles in the SLNC. The high percentage of individual particles <4 µm that is evidenced in the APSD (classes #2 to #6, Fig. 9B) systematically did not appear in the EPSD (Fig. 9A), suggesting that these small grains are systematically aggregated. The APSD do not contain particles of diameters >60 µm,, whereas EPSD curves display a distinct mode for particles of diameter >60 µm. Therefore, the presence of important volume concentration of particles >60 µm EPSD is entirely due to aggregates.

4.2.2.2. Characterization of aggregates. Visual checks were made to ensure that the coarsest particles were not plankton that could have been dislocated by sonification. Some of the water sampled *in situ* was poored in settling columns and visualized with an inverted microscope. Despite the differences that may occur in the visualized PSD

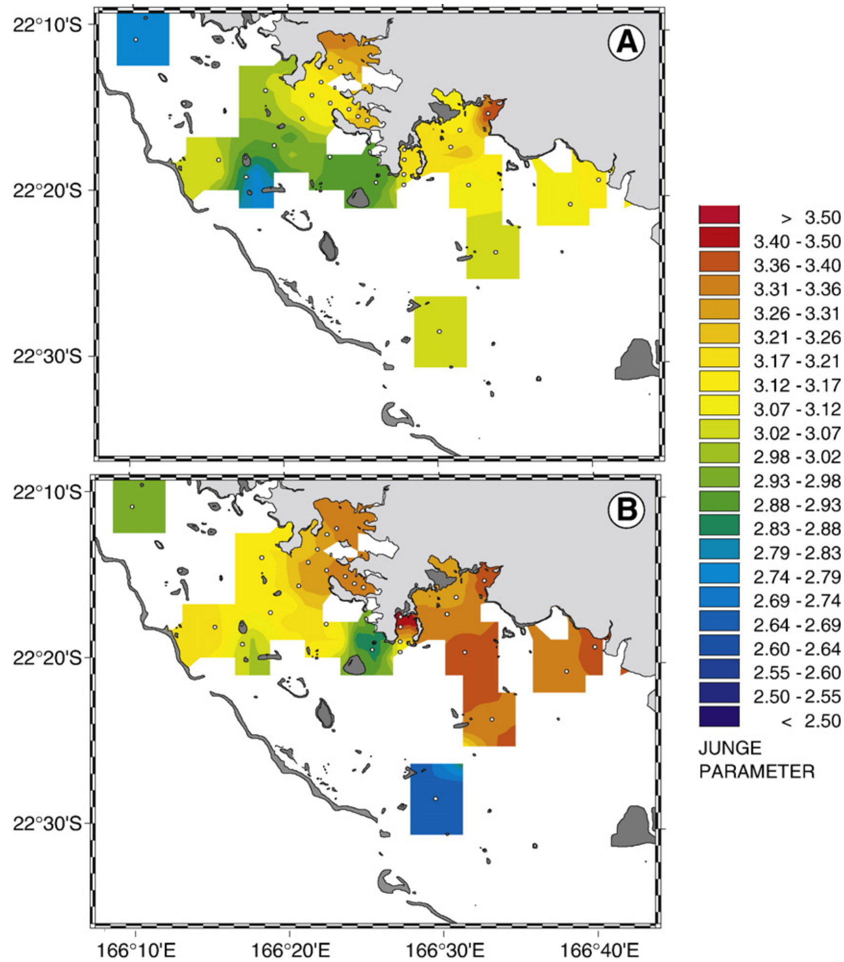

Fig. 8. Distribution of the Junge parameter: (A) in the surface layer (averaged from 3 m to 5 m below the sea surface), (B) in the bottom layer (averaged over 2 m depth).

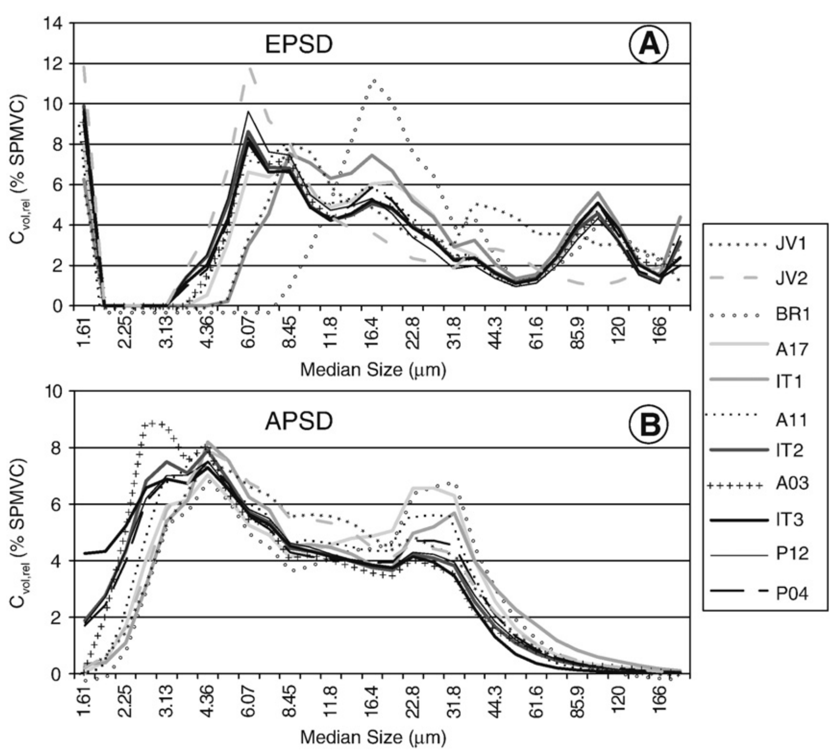

Fig. 9. EPSD (A) and APSD (B) at the same stations.

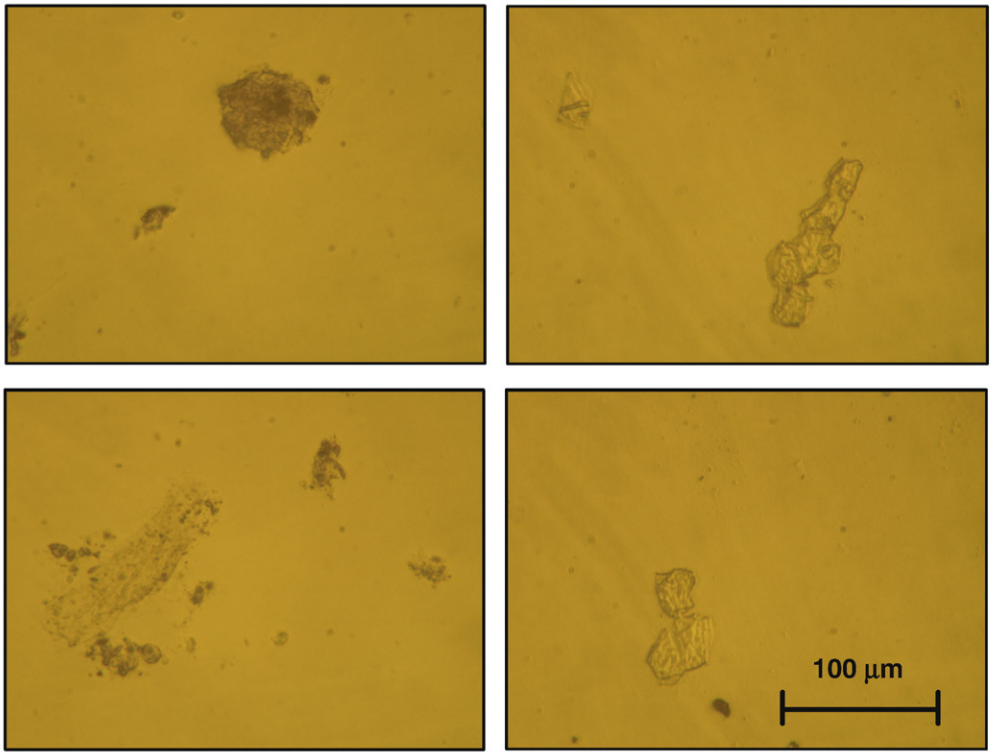

Fig. 10. Microscopic view of suspended particles. Sample from M12 on the 2005/09/21.

and the EPSD due to handling of the sample, the nature of constituent particles is identical. Fig. 10 shows examples of most frequently visualized particles: the coarser particles have a maximum length between 50 and 100 µm. They appear as aggregates of particles, a translucid matrix is most often dominant.

Chemical analysis was performed on a sample collected in the Boulari Bay on 2006/02/13 (Fig. 11). This analysis was achieved through the use of a Xray sensor mounted on an electron scanning microscope. The chemical analysis gives the nature and relative quantity of each element contained in a designated surface on the sample. The composition of matter contained on the part of the filter designated by the image shows a dominant terrigenous matter (Fe, Mg, Si, Al) with marine carbonate particles (Ca) and high content in organics (C, O). The diffuse dark stains on the image of Fig. 11 are almost exclusively made of organic matter.

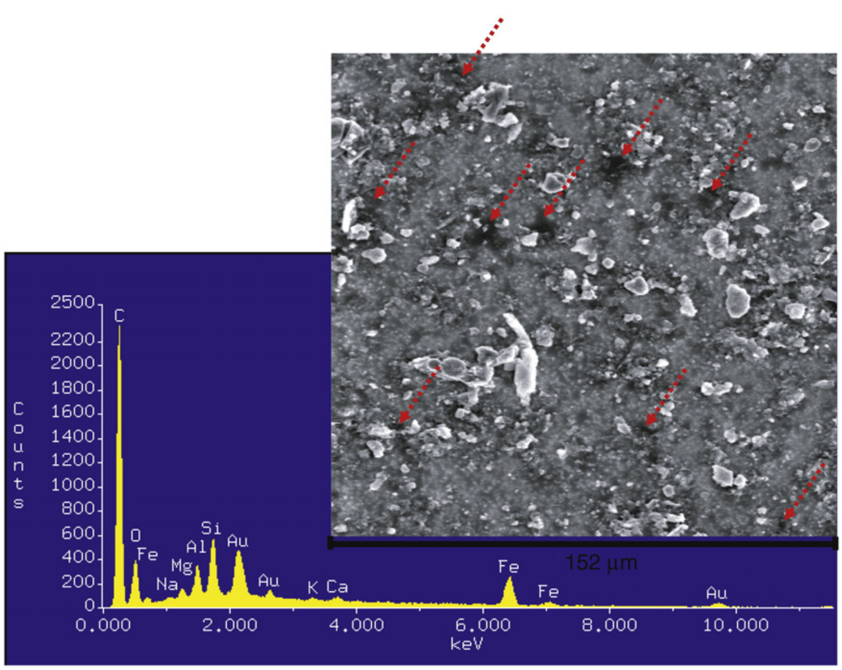

Fig. 11. Scanning electron microscope view and chemical analysis of filtered particles. Sample taken on the 2006/02/13 in Boulari Bay. Red arrows indicate organic rich stains on the filter.

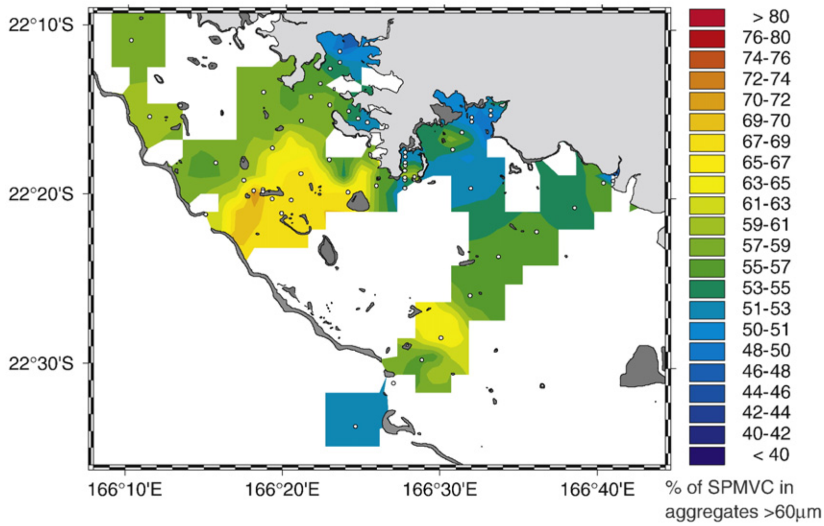

Fig. 12. Percentage of SPM volume concentration in aggregates of diameter >60 µm.

4.2.2.3. Aggregates' contribution to suspended particulate matter volumetric concentration. The percentage of SPMVC contained in aggregates >60 µm always exceeded 38% on the SLNC (Fig. 12). Higher values of relative abundance of large aggregates (~70%) were found in the surroundings of the barrier reef and coral islands. The percentage of volume concentration contained in aggregates >60 µm was higher than 45% all along the transect survey stations (Fig. 13). While the SPMVC increased from the reef to the coast, the percentage of suspended particles in aggregates >60 µm decreased.

5. Discussion

5.1. Suspended particulate matter volumetric concentration

The mean distribution of SPMVC on the SLNC is characterized by a major reef to coast gradient (Fig. 4) which is in fair agreement with turbidity distributions obtained from satellite data, field measurements and modeling exercises conducted in October 2002 (Ouillon et al., 2004). The variability of SPMVC is significant over space and time. The computed coefficient of variability over space includes some short-term variability. An estimate of the scale of this short-term variability showed that it could be neglected. Results have shown that the quantity of suspended particles on the SLNC was relatively more variable throughout the lagoon at a given moment than at a specific location throughout time in usual weather conditions (i.e. except during storms that were not sampled). Within the water depth, all optical measurements showed a net increase of SPM in the bottom nepheloïd layer, especially high in the bays around the Nouméa Peninsula (Fig. 5). Although the quantity of particle inputs to the SLNC have increased during the past century, the extent and volume of this nepheloïd layer is much smaller than in the GBR located 1500 km West from New Caledonia (Wolanski et al., 2003b).

In the SLNC, benthic sediments are the main source of suspended particles through resuspension (Clavier et al., 1995). Resuspension is governed by the availability of particles at the seabed, their erodibility properties, and the bottom shear stress whose variability is mainly constrained by the bathymetry variations (Douillet et al., 2001). In an optimization exercise involving a numerical model and turbidity measurements, Ouillon et al. (2004) showed that terrigenous sediments were more easily erodible than biogenic carbonate sediments in the SLNC. In her study on sewage muds, Tixier (2003) demonstrated that carbonates are more cohesive than terrigenous silicate particles of same diameter. As the terrigenous sediments dominates in the vicinity of river mouths (Debenay, 1987; Chardy et al., 1988), the mean distribution of SPMVC show the highest values in Dumbea Bay and in Boulari Bay were sediments that are more easily eroded. In areas of higher residence time, as in Grande Rade and in the Sainte-Marie Bay, Mari et al. (2007) proved that aggregates included older organic matter leading to a lower density of aggregates. The high values of SPMVC inside these bays could also be due to a slower settling of particles than in other parts of the lagoon where residence time is lower (Jouon et al., 2006).

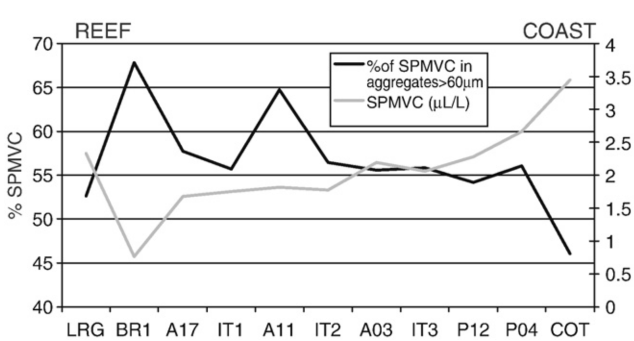

Fig. 13. SPMVC and Percentage of SPM volume concentration in aggregates of diameter >60 µm along a coast-large transect.

5.2. Variability of EPSD: aggregation processes

Even if it bears some of the short-term variability of EPSD, the standard deviation of relative EPSD over space can be considered as a significant index of space variability of EPSD. It was found to be lower than the standard deviation of relative EPSD over time suggesting that, contrary to the volume concentration of particles, long term (monthly) variability of the effective particle size distribution was higher than its spatial variability.

The disaggregating experiments showed that *in situ* particles with diameter over 60 µm were aggregates. The particles smaller than 60 µm observed during field measurements were composed of an undetermined fraction of aggregates. Considering that particles of diameter >60 µm represent all aggregates gives us a low estimate of the state of aggregation of EPSD. This low estimation still represents a significant fraction of the volume concentration (40 to 90%, Fig. 12).

The comparisons of dispersed APSDs to EPSDs show that particles <4 µm are systematically aggregated. The highest values of standard deviations over space and time in the EPSD (class #7, see Fig. 7) coincide with the upper size limit of the single particles showing a strong propensity to be aggregated (Fig. 9). These high standard deviations are encountered for the particle sizes at the boundary between the most abundant (6 μm) and the most rare (<3 μm) effective natural particle sizes, suggesting a shift from small particles (<3 μm) to larger due to aggregation. Moreover, as APSDs show that there were no individual grains >60 μm in SPM (Fig. 9b), the peaks in standard deviation of PSD over space and time for size ~100 μm (Fig. 7) concern aggregates and are likely due to aggregation/disaggregation processes. These two points suggest that aggregation significantly influences the variability of EPSD.

Figs. 5 and 6 indicate that, the proportion of large particles (aggregates) is higher in the upper and less turbid waters.

5.3. Quantifying SPM from optical measurements

The obtained values of determination coefficient are low, which indicates that the relationship between mass concentration and bulk optical measurements of SPM is not straightforward.

The slope of the linear regression relationship between turbidity and mass concentration is about 85% higher than that usually used in turbid estuaries (e.g. Jin et al., 2001). This slope was shown to be strongly dependent of the particle diameter and gets steeper with decreasing diameter (Bunt et al., 1999).

The comparison of correlation between OBS signal and each class of the EPSD highlights that turbidity is more sensitive to the smallest particles (between 2 and 22 μm, see Fig. 3) (Bunt et al., 1999; Creed et al., 2001). This result supports previous results suggesting a correction of OBS signal to derive SPM concentration by taking into account the median diameter of EPSD (e.g. Lynch et al., 1994). Aggregation increases the mean diameter of particles and was already shown to be responsible for lowering the turbidity signal at an equal mass concentration (Gibbs and Wolanski, 1992). The variability of the percentage of aggregates (Fig. 12) thus likely explains the low determination coefficient obtained between turbidity and mass concentration (Fig. 2) as compared to determination coefficient reported in some other coastal zones.

The highest correlations between beam attenuation at 670 nm and volume concentration were found at two intervals of LISST data EPSD (Fig. 3). The first size range to which c670 is more sensitive (3 to 5 μm) is in accordance with previously published results: beam attenuation increases with decreasing mean grain size at the same SPM up to 14-fold (Baker and Lavelle, 1984; Boss et al., 2001a,b). A second interval of even better correlation between c670 and LISST data EPSD concerns particles in classes #22 to #26 (~40 to 100 μm). These size classes correspond approximately to the smallest particles identified as aggregates: these particles may not be too large to efficiently attenuate light and they are also well represented in the SPM pool.

However, the present correlations show that, contrary to the previous version of LISST, the LISST-100X provides reliable measurements between 2 and 5 μm.

The lowering of correlation for the large bin sizes of LISST can be interpreted as a negligible contribution of the coarse particles to turbidity and mass concentration. This suggests that coarser particles backscatter light less efficiently and have a lower density.

Unlike turbidity and beam attenuation signals, LISST measurements of volume concentration are not dependent upon the particle size distribution but they are restricted to particles with diameter comprised between 1.48 and 213 μm, whereas mass concentration is determined for all particles >1 μm.

The imprecision of LISST at extreme values and the exclusion of these values from the analysis is a potential source of error. Creed et al. (2001) used another version of LISST-100 which has a sensing window that extends from 1.25 to 500 μm. They reported the inability of the instrument to correctly measure sediment of grain size >250 μm (which included the top four bins of their LISST's version) and <5 μm. Furthermore, the contribution of noise to the measurement limits to about 10-12 the number of sizes classes that may be resolved through the 200:1 size range observable by this instrument (Sequoia Scientific Inc., 2001). Each size class measurement is thus not entirely independent from the adjacent size class value. As a result, more than a single size class could be excluded from computations at the boundaries of LISST-100X sensing range.

In the present study, extremely weak correlations were obtained for the outlying size classes which supports our decision to exclude these bins from other computations.

Another potential source of discrepancy in the determination coefficient between mass and volume concentrations may be linked to the LISST data processing. A unique constant is used to calculate the volume concentration of particles from the intensity of diffracted light in every size class. This constant is determined experimentally by the manufacturer. First studies which used LISST with a single volume conversion constant underlined the accuracy of such processing (Traykovski et al., 1999; Agrawal and Pottsmith, 2000). However, Gartner et al. (2001) demonstrated that the instrument dependent constant was also class dependent. The results displayed in Mikkelsen et al. (2005) also suggest the class dependency of the volume conversion constant.

The variability of density of sensed particles could also explain discrepancies in the mass to volume concentration ratio. Biogenic and terrigenous particles do not strictly have the same density. Given the abundance of aggregates in the study area, the variation of density could be mainly attributed to the variability of aggregate density and to the variability of the state of aggregation of EPSD.

Results show that aggregates are dominant constituents of SPM. Under the conditions of having a much larger volume of water compared to the volume of solid grains in the aggregates, Mikkelsen and Pejrup (2001) proposed the following relation to determine the mean density of suspended aggregates:

$$\Delta\rho = \rho_F - \rho_W \approx \frac{TSM}{SPMVC} \tag{8}$$

where $\Delta\rho$ is the aggregate's effective mean density, ρ_W is the water density (ρ_W=1.02 kg L^{-1} is considered in the calculation), ρ_F is the density of aggregates, and TSM is Total Suspended Matter mass concentration. The linear regression between SPMVC and mass concentration yields a slope coefficient equal to 4.0 μL mg^{-1} (Fig. 2a). Considering for this computation that all sensed particles are aggregates, the corresponding $\Delta\rho$ is thus 0.25 kg L^{-1}, which provides mean density of equivalent aggregates over the sampling scheme ρ_F=1.27 kg L^{-1}. The computed value of mean particle density is lower than terrigenous grain's density, but higher than the high range of aggregates densities given in Mikkelsen and Pejrup (2001) (ρ_F=1.037 to 1.194 kg L^{-1}).

5.4. An insight into aggregation process regulation

Although the suspended particle concentration was very low in the coral reef lagoon of New Caledonia, aggregation was shown to be significant.

The size, density and strength of aggregates are dependent on the total amount of suspended sediments, suspension residence time, turbulence, salinity, temperature, coatings on particles surfaces, dissolved organic substances, and biological organisms (Voulgaris and Meyers, 2004). The amount of aggregates over total SPM and the size of the aggregates are continuously changing and determined by aggregation and disaggregation processes (Chaignon et al., 2002). The time scale of aggregation is generally considered to be short (Gibbs and Wolanski, 1992; Wolanski et al., 2003a). Gratiot and Manning (2004) show that it takes about 30 min for a dense suspension to reach the equilibrium under turbulent conditions in a laboratory. Since this time scale of aggregation was not inferred from our measurements in the SLNC, we may only consider as a first step that the state of aggregation is in equilibrium with the surrounding parameters.

Two fundamental conditions must be fulfilled for aggregation to take place: first, particles must collide and second, they must adhere (van Leussen, 1994). The frequency of collisions increases when the concentration of suspended particles is high. Working on activated sludge, Chaignon et al. (2002) demonstrated a linear relation between the mass concentration of sludge and the mean aggregate size. In this study, the depth-profile of EPSD showed a lesser percentage of aggregates in the bottom nepheloïd layer, which is somewhat contradictory to the dependency of aggregation processes on the SPM mass concentration (Fig. 5). This result is also in opposition with the tendency observed in the Mid-Atlantic Bight where the spectral shape of EPSD is steeper when distance to the bottom increases (Boss et al., 2001b). The observed increase of volume concentration and lowering of the relative quantity of aggregates on a reef to coast transect also seems paradoxical with the dependency of aggregation processes on the SPM concentration (Fig. 13).

Among mechanisms known to promote collision (Brownian motion, turbulence, and differential sedimentation) and to induce breaking of aggregates (Alldredge et al., 1990; van Leussen, 1994; Chaignon et al., 2002), turbulence is a key hydrodynamic parameter. As turbulence was not measured during our field campaigns, we explored the sensitivities of EPSD to sea level speed of variation (as proxy of turbulence induced by the tide) and to wind velocity (as a proxy of turbulence induced by the wind), but found no significant relationships.

The "stickiness" of aggregates is another important parameter to determine the aggregate size. The stickiness of a single particle is determined by two primary mechanisms: electrostatic forces, considered to be the most common interaction responsible for inorganic particle coagulation (Voulgaris and Meyers, 2004), and biological activity (van Leussen, 1994).

Having shown that SPMVC is low on the barrier reef side of the lagoon and that the percentage of aggregates is higher in these areas, this study suggests that stickiness is a contributing factor for the state of aggregation of EPSD on the SLNC.

Organic matter improves the stickiness of aggregates (Gratiot and Manning, 2004). Many studies focusing on biologically aggregated flocs (i.e. organic aggregates) emphasize the importance of exopolymeric substances as the main floc forming constituent (Chaignon et al., 2002; Mikkelsen and Keiding, 2002a,b; Thornton, 2002; Tixier, 2003; Wolanski et al., 2003a; Sheng et al., 2006). Exopolymeric substances originate from marine life metabolism or cell lyses. Transparent Exopolymeric Particles (TEP) are formed by coagulation of exopolymeric substances, and are positively buoyant particles that have been shown to regulate the buoyancy of aggregates (Azetsu-Scott, 2004). On the SLNC, Mari et al. (2007) show that aggregates remain in suspension after prolonged steady calm conditions and explain their low fall velocity by the inclusion of TEP in the aggregates. The visualization of aggregates through a microscope showed that an important volume of aggregates was filled with a translucid matrix. The result of chemical analysis supports that carbon is a major constituent of suspended particles on the SLNC. These two observations support the conclusions of Mari et al. (2007) regarding the presence of TEP inside the SPM pool. In a system dominated by mineral particles, aggregation is often associated with an increase in settling velocity (van Leussen, 1994; Winterwerp, 2002; Gratiot et al., 2005). The low settling velocity observed by Mari et al. (2007) discredit the assumption used in previous studies of particle transport on the SLNC of an inorganic particle dominated environment. Furthermore, the estimated aggregate density (1.27 g cm^{-3}) is in accordance with the range of measured densities for solid matter of large aggregates cited in Mari et al. (2007) (i.e., from 1.095 to 1.497 g cm^{-3}, values given in a review by Azetsu-Scott and Johnson, 1992).

The monthly variability of EPSD computed in this study was higher than their 24 hour-variability or spatial variability. The time scale variations of EPSD does not seem to be connected to the time scales of the major physical forcings which take place on the SLNC.

Spatially, the higher percentage of aggregates in the SLNC are found in the surroundings of the barrier reef and around coral islands. Coral ecosystems are known to release large amounts of exopolymeric substances (i.e., up to 4.8 L of mucus per day per square meter of coral reef, Wild et al., 2004). The abundance of exopolymeric substances in corals environments may enhance overall sticking properties of suspended particles and, thus, raise the critical level of turbulence necessary to break aggregates apart. This assumption is consistent with previous observations of enhanced aggregation and reduced settling velocity around coral reefs: Wolanski et al. (2003a) brought to light low settling velocities for aggregates occurring in a reef fringed bay and argued that these low settling velocities were best explained by the inclusion of TEP in the composition of aggregates; the flocculation catalyzed by the proximity of a coral reef was also a plausible explanation for the conclusions obtained in Hoitink (2004): "Coral reefs create a distinct sedimentary regime in their surroundings, sediments transported towards coral reef environments do not address local turbidity variation".

Finally, all these elements bring up the hypothesis of biological aggregation as an important process in suspended particle transport in coral environments.

6. Conclusion

The dependence of the beam attenuation coefficient and turbidity to the particle size distribution was highlighted. Both parameters increase with decreasing mean grain size (Baker and Lavelle, 1984; Mikkelsen and Pejrup, 2000; Boss et al., 2001b). As the state of aggregation may be altered during sample handling, the calibrations of beam attenuation measuring devices and OBS have to be done *in situ*. Even then, the importance and the variability of the state of aggregation of EPSD lead to important fluctuations in the signal to mass ratio for both devices. OBS and c670 measurements may not be suitable to properly quantify SPM in environments where large particles and/or aggregates dominate (Creed et al., 2001). As OBS are less sensitive to large aggregates than to individual grains, disaggregation can potentially lead to increased turbidity (Mikkelsen and Keiding, 2002b), and may lead to misinterpretation of functioning of studied systems (Ellis et al., 2004).

Although inputs of sediments to the SLNC have increased over the last century, SPM exhibits very low concentration (0.1 to 8 mg L^{-1}). A high percentage of aggregates (45 to 75%) compose the SPM. This percentage varies significantly, with higher variations at a monthly-scale than over space as well as over 24 h in non-extreme weather conditions. Knowing that OBS devices and beam attenuation factors are particle size sensitive, the dynamic of the state of aggregation can lead to variations in the measurement of suspended particle load. Standing on previously published observations (Mari et al., 2007) and relying on visual observations of the aggregates as well as an analysis of the chemical composition of one sample, biological aggregation seems to have a dominant impact on the EPSD in the SLNC. Despite a lack of measurements of physical forcings such as turbulence, the spatial extent of our study allowed us to identify an increase of aggregate percentage in the surroundings of coral reefs. The hypothesis is offered that aggregation could be catalyzed by the proximity of coral ecosystems. The catalyzation of biological aggregation in the surroundings of a coral ecosystem would affect the fate of all suspended particulate matter in all coral environments.

Acknowledgments

This work was supported by the New Caledonian "ZoNéCo" program, by the French BISSECOTE program ("ACI Observation de la Terre"), and by the French "Programme National Environnement Côtier". The authors warmly thank Jean-Pierre Lamoureux who measured dry weight of particles, Sam Tereua, Napoléon Colombani, Miguel Clarke and the crew of N.O. Alis for their contribution to the field measurements.

References

Achite, M., Ouillon, S., 2007. Suspended sediment transport in a semiarid watershed, Wadi Abd, Algeria (1973–1995). J. Hydrol. 343, 187–202.

Agrawal, Y.C., Pottsmith, H.C., 2000. Instrument for particle size and settling velocity observations in sediment transport. Mar. Geol. 16, 89–114.

Alldredge, A.L., Granata, T.C., Golschalk, C.C., Dickey, T.D., 1990. The physical strength of marine snow and its implications for particle disaggregation in the ocean. Limnol. Oceanogr. 35, 1415–1428.

Azetsu-Scott, K., 2004. Ascending marine particles: Significance of transparent exopolymer particles (TEP) in the upper ocean. Limnol. Oceanogr. 49, 741–748.

Azetsu-Scott, K., Johnson, B.D., 1992. Measuring physical characteristics of particles: a new method of simultaneous measurement for size, settling velocity and density of constituent matter. Deep-Sea Res. 39, 1057–1066.

Babcock, R., Davies, P., 1991. Effects of sedimentation on settlement of *Acropora millepora*. Coral Reefs 9, 205–208.

Baker, E.T., Lavelle, J.W., 1984. The effect of particle size on the light attenuation coefficient of natural suspensions. J. Geophys. Res. 89, 8197–8203.

Benson, A.A., Muscatine, L., 1974. Wax in coral mucus: Energy transfer from coral to fishes. Limnol. Oceanogr. 19, 810–814.

Bird, E.F.C., Dubois, J.P., Iltis, J.A., 1984. The Impacts of Opencast Mining on the Rivers and Coasts of New Calodonia. United Nations University, Tokyo.

Bonneton, P., Lefebvre, J.P., Bretel, P., Ouillon, S., Douillet, P., 2007. Tidal modulation of wave-setup and wave-induced currents on the Aboré coral reef, New Caledonia. J. Coast. Res. 50 (SI), 762–766.

Boss, E., Twardowski, M.S., Herring, S., 2001a. Shape of the particulate beam attenuation spectrum and its inversion to obtain the shape of the particulate size distribution. Appl. Opt. 40, 4885–4893.

Boss, E., Pegau, W.S., Gardner, W.D., Zaneveld, J.R.V., Barnard, A.H., Twardowski, M.S., Chang, G.C., Dickey, T.D., 2001b. Spectral particulate attenuation and particle size distribution in the bottom boundary layer of a continental shelf. J. Geophys. Res. 106, 9509–9516.

Bunt, J.A.C., Larcombe, P., Jago, C.F., 1999. Quantifying the response of optical backscatter devices and transmissometers to variations in suspended particulate matter. Cont. Shelf Res. 19, 1199–1220.

Chaignon, V., Lartigues, B.S., El Samrani, A., Mustin, C., 2002. Evolution of size distribution and transfer of mineral particles between flocs in activated sludges: an insight into floc exchange dynamics. Water Res. 36, 676–684.

Chardy, P., Chevillon, C., Clavier, J., 1988. Major benthic communities of the south-west lagoon of New Caledonia. Coral Reefs 7, 69–75.

Clavier, J., Chardy, P., Chevillon, C., 1995. Sedimentation of particulate matter in the south-west lagoon of New Caledonia: spatial and temporal patterns. Estuar. Coast. Shelf Sci. 40, 281–294.

Creed, E.L., Pence, A.M., Rankin, K.L., 2001. Inter-comparison of turbidity and sediment concentration measurements from an ADP, an OBS-3, and a LISST. Oceans 2001, Proc. MTS/IEEE conf. 3, pp. 1750–1754.

Curran, K.J., Hill, P.S., Milligan, T.G., Mikkelsen, O.A., Law, B.A., Durrieu de Madron, X., Bourrin, F., 2007. Settling velocity, effective density, and mass composition of suspended sediment in a coastal bottom boundary layer, Gulf of Lions, France. Cont. Shelf Res. 27, 1408–1421.

Debenay, J.P., 1987. Sedimentology in the south-west lagoon of New Caledonia, SW Pacific. J. Coast. Res. 3, 77–91.

Douillet, P., 1998. Tidal dynamics of the south-west lagoon of New Caledonia: observations and 2D numerical modelling. Oceanol. Acta 21 (1), 69–79.

Douillet, P., Ouillon, S., Cordier, E., 2001. A numerical model for fine suspended sediment transport in the southwest lagoon of New Caledonia. Coral Reefs 20, 361–372.

Droppo, I.G., 2001. Rethinking what constitutes suspended sediments. Hydrol. Proced. 15, 1551–1564.

Ellis, K.M., Bowers, D.G., Jones, S.E., 2004. A study of temporal variability in particle size in a high-energy regime. Estuar. Coast. Shelf Sci. 61, 311–315.

Ellison, J.C., 1999. Impacts of sediment burial on mangroves. Mar. Pollut. Bull. 37 (8-12), 420–426.

Fabricius, K.E., Wild, C., Wolanski, E., Abele, D., 2003. Effects of transparent exopolymer particles and muddy terrigenous sediments on the survival of hard coral recruits. Estuar. Coast. Shelf Sci. 57, 613–621.

Fernandez, J.M., Ouillon, S., Chevillon, C., Douillet, P., Fichez, R., Le Gendre, R., 2006. A combined modelling and geochemical study of the fate of terrigenous inputs from mixed natural and mining sources in a coral reef lagoon (New Caledonia). Mar. Poll. Bulletin 52, 320–331.

Forget, P., Ouillon, S., Lahet, F., Broche, P., 1999. Inversion of reflectance spectra of nonchlorophyllous turbid coastal waters. Rem. Sensing Env. 68, 264–272.

Fugate, D.C., Friedrichs, C.T., 2002. Determining concentration and fall velocity of estuarine particle populations using ADV, OBS and LISST. Cont. Shelf Res. 22, 1867–1888.

Fugate, D.C., Friedrichs, C.T., 2003. Controls on suspended aggregate size in partially mixed estuaries. Estuar. Coast. Shelf Sci. 58, 389–404.

Gartner, J.W., Cheng, R.T., Wang, P.F., Richter, K., 2001. Laboratory and field evaluations of the LISST-100 instrument for suspended particle size distributions, Mar. Geol. 175 (1-4), 199–219.

Gentien, P., Lunven, M., Lehaître, M., Duvent, J.L., 1995. *In-situ* depth profiling of particle sizes. Deep-Sea Res. 42, 1297–1312.

Gibbs, R.J., 1982. Floc stability during Coulter-Counter size analysis. J. Sediment. Petrol. 52, 657–660.

Gibbs, R.J., Wolanski, E., 1992. The effect of flocs on optical backscattering measurements of suspended material concentration. Mar. Geol. 107 (4), 289–291.

Gratiot, N., Manning, A.J., 2004. An experimental investigation of floc characteristics in a diffusive turbulent flow. J. Coast. Res. SI41, 105–113.

Gratiot, N., Michallet, H., Mory, M., 2005. On the determination of the settling flux of cohesive sediments in a turbulent fluid. J. Geophys. Res. 110, C06004.

Hayward, A.B., 1982. Coral reefs in a clastic sedimentary environment: fossils (Miocene, SW Turkey) and modern recent (Red Sea) analogues. Coral Reefs 1, 109–114.

Hoitink, A.J.F., 2004. Tidally-induced clouds of suspended sediment connected to shallow-water coral reefs. Mar. Geol. 208, 13–31.

Hopley, D., 1994. Continental reef systems. In: Carter, R.W.G., Woodroffe, C.D. (Eds.), Coastal Evolution: Late quaternary shoreline Morphodynamics. Cambridge Univ. Press, Cambridge, pp. 303–340.

Jin, J.Y., Lee, D.Y., Park, J.S., Park, K.S., Yum, K.D., 2001. Monitoring of suspended sediment concentration using vessels and remote sensing. In: McAnally, W.H., Mehta, A.J. (Eds.), Coastal and Estuarine Fine Sediment Processes. Elsevier, Amsterdam, The Netherlands, pp. 287–299.

Johannes, R.E., 1967. Ecology of organic aggregates in the vicinity of a coral reef. Limnol. Oceanogr. 12, 189–195.

Jouon, A., Douillet, P., Ouillon, S., Fraunié, P., 2006. Calculations of hydrodynamic time parameters in a semi-opened coastal zone using a 3D hydrodynamic model. Cont. Shelf Res. 26, 1395–1415.

Larcombe, P., Ridd, P.V., Prytz, A., Wilson, B., 1995. Factors controlling suspended sediment on innershelf coral reefs, Townsville, Australia. Coral Reefs 14, 163–171.

Lynch, J.F., Irish, J.D., Sherwood, C.R., Agrawal, Y.C., 1994. Determining suspended sediment particle size information from acoustical and optical backscatter measurements. Cont. Shelf Res. 14, 1139–1165.

Mari, X., Rochelle-Newall, E., Torréton, J.P., Pringault, O., Jouon, A., Migon, C., 2007. Water residence time: a regulatory factor of the DOM to POM transfer efficiency. Limnol. Oceanogr. 52, 808–819.

Migon, C., Ouillon, S., Mari, X., Nicolas, E., 2007. Geochemical and hydrological constraints on the distribution of trace metal concentrations in the lagoon of Noumea, New Caledonia. Est. Coastal Shelf Sci. 74 (4), 657–666.

Mikkelsen, O.A., Pejrup, M., 2000. In situ particle size spectra and density of particle aggregates in a dredging plume. Mar. Geol. 170, 443–459.

Mikkelsen, O.A., Pejrup, M., 2001. The use of LISST-100 in-situ laser particle sizer for estimates of floc size, density and settling velocity. Geo Mar. Lett. 20, 187–195.

Mikkelsen, L.H., Keiding, K., 2002a. Physico-chemical characteristics of full scale sewage sludges with implication to dewatering. Water Res. 36, 2451–2462.

Mikkelsen, L.H., Keiding, K., 2002b. The shear sensitivity of activated sludges: an evaluation of the possibility for a standardised floc strength test. Water Res. 36, 2931–2940.

Mikkelsen, O.A., Hill, P.S., Milligan, T.G., Chant, R.J., 2005. In situ particle size distributions and volume concentrations from a LISST-100 laser particle sizer and a digital floc camera. Cont. Shelf Res. 25, 1959–1978.

Mobley, C.D., 1994. Light and Water Radiative Transfer in Natural Water. Academic Press, San Diego. 592 pp.

Ouillon, S., Douillet, P., Andréfouët, S., 2004. Coupling satellite data with in situ measurements and numerical modeling to study fine suspended sediment transport: a study for the lagoon of New Caledonia. Coral Reefs 23, 109–122.

Ouillon, S., Douillet, P., Fichez, R., Panché, J.Y., 2005. Enhancement of regional variations in salinity and temperature in a lagoon, New Caledonia. CR Geosci. 337, 1509–1517.

Rogers, C.S., 1990. Responses of coral reefs and reef organisms to sedimentation. Mar. Ecol. Prog. Ser. 62, 185–202.

Sequoia Scientific Inc., 2001. The Size Resolution of the LISST Series of Instruments, Application note L008. 2 pp.

Sheng, G.P., Yu, H.Q., Li, X.Y., 2006. Stability of sludge flocs under shear conditions: role of extracellular polymeric substances (EPS). Biotech. Bioeng. 93, 1095–1102.

Thornton, D.C.O., 2002. Diatom aggregation in the sea: mechanism and ecological implications. Eur. J. Phycol. 37, 149–161.

Tixier, N., 2003. Approche des propriétés rhéologiques de suspensions biologiques floculées. Ph.D. Thesis. Univ. Limoges, France.

Torréton, J.-P., Rochelle-Newall, E., Jouon, A., Faure, V., Jacquet, S., Douillet, P., 2007. Correspondence between the distribution of hydrodynamic time parameters and the distribution of biological and chemical variables in a semi-enclosed coral reef lagoon. Estuar. Coast. Shelf Sci. 74 (4), 667–677.

Traykovski, P., Latter, R., Irish, J.D., 1999. A Laboratory Evaluation of the LISST Instrument Using Natural Sediments. Mar. Geol. 159, 355–367.

van Leussen, W., 1994. Estuarine Macroflocs and their role in fine grained sediment transport. PhD Thesis, University of Utrecht.

Voulgaris, G., Meyers, S.T., 2004. Temporal variability of hydrodynamics, sediment concentration and sediment settling velocity in a tidal creek. Cont. Shelf Res. 24, 1659–1683.

Wass, P.D., Marks, S.D., Finch, J.W., Leeks, G.J.L., Ingram, J.K., 1997. Monitoring and preliminary interpretation of in-river turbidity and remote sensing imagery for suspended sediment transport studies in the Humber catchment. Sci. Total Environ. 194/195, 263–283.

Wild, C., Huettel, M., Klueter, A., Kremb, S.G., Rasheed, M.Y.M., Jorgensen, B.B., 2004. Coral mucus as an energy carrier and particle trap in the reef ecosystem. Nature 428, 66–70.

Williams, N.D., Walling, D.E., Leeks, G.J.L., 2007. High temporal resolution in situ measurement of the effective particle size characteristics of fluvial suspended sediment. Water Res. 41 (5), 1081–1093.

Winterwerp, J.C., 2002. On the flocculation and settling velocity of estuarine mud. Cont. Shelf Res. 22, 1339–1360.

Wodzicki, K., 1981. Some nature conservation problems in the South Pacific. Biol. Conserv. 21, 5–18.

Wolanski, E., Richmond, R.H., Davis, G., Bonito, V., 2003a. Water fine sediment dynamics in a transient river plumes in a small, reef-fringed bay, Guam. Estuar. Coast. Shelf Sci. 56, 1029–1040.

Wolanski, E., Marshall, K., Spagnol, S., 2003b. Nepheloid layer dynamics in coastal waters of the Great Barrier Reef, Australia. J. Coast. Res. 19 (3), 748–752.